Subpicosecond Kinetic Polarization Spectroscopic Study of the Complex Photophysical Behavior of Solutions of 9,9′-Bianthryl

Erik J. A. de Bekker, Audrius Pugzlys, and Cyril A. G. O. Varma*

Leiden Institute of Chemistry, Leiden University, Gorlaeus Laboratories, P.O. Box 9502, 2300 RA Leiden, The Netherlands

Received: July 12, 2001; In Final Form: February 20, 2002

Several new aspects of the complex photophysical behavior of solutions of 9,9′-bianthryl are reported. They have been revealed by the time dependencies of the depolarization of the fluorescence and the photoinduced transient optical absorptions of these solutions. A comparison is provided with the depolarization kinetics in the case of solutions of anthracene. The observed depolarization behavior is interpreted on the basis of a theoretical treatment which is presented in some detail. The main conclusions are summarized at the end of the publication.

Introduction

Optical spectroscopy in the ultraviolet and visible wavelength region of the spectrum has proven to be a powerful tool in the study of chemical reactivities in the liquid state. Thorough understanding of the spectroscopic consequences of solute−solvent interactions is of prime importance in this field to arrive at reliable interpretations of the observations. It is therefore worthwhile to gather knowledge which may lead to full understanding of yet incompletely explained spectroscopic observations such as those encountered in the spectroscopic studies of solutions of 9,9′-bianthryl (BA)[1]. Many interesting details have already been discovered concerning the behavior of electronically excited BA dissolved in nonpolar and polar solvents. Attention has been strongly focused on the dual fluorescence of solutions of BA in polar solvents. The fluorescence spectrum of these solutions consists of two bands, namely the normal band F_N at short wavelengths, resembling the only band appearing in the case of solutions in e.g. alkanes, and an anomalous band F_A at much longer wavelengths. The primary excited state of BA in nonpolar solvents, prepared by photoexcitation within the first UV-absorption band, has no permanent dipole moment and its polarizability differs from that in the ground state by the same amount as the difference between excited state and ground-state polarizability of a single anthracene molecule.[2,3] Although this is to be expected, the observed fluorescence of solutions of BA in alkanes cannot be interpreted easily. The temperature dependence of the fluorescence spectrum revealed that the reason for this is that various forms of the excited solute emerge from the primary excited state.[4] The fluorescent states of BA in several nonpolar solvents have been found to lead to transient dielectric loss at microwave frequencies. The variations in the losses with changes of solvent have been attributed to the orientational relaxation of solute−solvent exciplexes with a dielectric relaxation time τ_D of at least 60 ps.[4] The reasoning has been based on the Debye theory of dielectric relaxation, which applies only when the loss is entirely caused by overall rotation of a rigid dipole. The term solute−solvent exciplex refers to an association of a ground state solvent molecule and an excited solute molecule that is stable during the time of observation, but becomes unstable when the solute returns to its ground state. The formation of 1:1 solute−solvent exciplexes of BA could be demonstrated clearly in the case of polar solvent molecules. Solutions of BA in alkanes with some additional polar solvent exhibit linear Stern Volmer quenching of the normal fluorescence F_N accompanied by a linear increase in the ratio $I(F_A)/I(F_N)$ of the intensities of the bands F_A and F_N with the concentration of polar solute. Evidence has been provided that the solute−solvent exciplex of BA in acetonitrile is the precursor of the radical cation of BA.[4]

The dielectric losses of photoexcited solutions of BA in nonpolar solvents have been reexamined,[5] and an attempt has been made to determine τ_D from the observed losses. The analysis of the results led to a value of τ_D that is far too small to be associated with overall rotation of excited BA. Therefore, the suggestion has been made that an intramolecular transition between two electronic states is involved in the microwave absorption. However, the method applied to determine τ_D is not consistent with this conclusion, because it relies on the dipole reorientation theory of Debye, while a quantum mechanical treatment is required in the case of intramolecular transitions. In the latter case the loss is depending on an electronic transition moment and not on a permanent dipole moment as in Debye's theory. Nevertheless, the studies of the transient dielectric losses reveal clearly the presence of polar species in the photoexcited solutions of BA in nonpolar solvents and that Debye's theory does not apply to the dielectric relaxation of these solutions.

The presence of polar species in photoexcited solutions of BA has also been detected by means of electric field modulation of their fluorescence spectra.[5] Serious difficulties have been encountered in the interpretation of these modulations in terms of dipole orientation and band shifts alone.[6] The involvement of solute−solvent exciplexes in the modulation effect could not be ruled out.[6] It seems that the electric field dependence of the chemical equilibrium between the bare excited solute and the solute−solvent exciplex (or any other polar form of BA) may have to be taken into account in the explanation of both the dielectric loss and the electric field modulation of the fluorescence.

* Corresponding author.

10.1021/jp012693r CCC: $22.00
Published on Web 06/04/2002

The fluorescence of BA in alkanes has been shown to arise from at least three different types of excited species, namely from the relaxed primary excited singlet state ($S_f^{(1)}$) and two other species ($S_f^{(2)}$ and $S_f^{(3)}$) in an equilibrium emerging from ($S_f^{(1)}$).[4] Despite this evidence, a number of recent explanations of the fluorescence behavior of solutions BA rely heavily on the assumption that the band F_N of solutions in an alkane can be considered as a band covering a single electronic transition.[7,8] An interesting attempt has been made to decompose fluorescence spectra of solutions of BA in several solvents into bands F_N and F_A by considering the fluorescence band of the solution in 1,3-dimethyl-perfluorocyclohexane (DMPFC) as arising from the bare excited solute molecule with negligible solute−solvent interaction.[9] However, two striking features went unnoticed. One is that the fluorescence is quenched dramatically in going from cyclohexane as the solvent to DMPFC. The quenching is most probably caused by electron transfer within solute−solvent exciplexes. The other feature is that a similar band structure is observed in the fluorescence spectra of the solutions in cyclohexane and in DMPFC, but the ratio of the heights of the peaks is significantly different. The peak at the shortest wavelength is substantially higher than its nearest neighbor at the long wavelength side in the case of the bare solute in cyclohexane.[4] These two peaks are of equal height in the case of the solution in DMFPC. A reasonable explanation for the discrepancy is that the latter spectrum does not emerge from a single type of species as has been assumed. As a consequence the solvatochromic shifts resulting from the decompositions may not be sufficiently accurate to determine the excited-state dipole moment of the species emitting the anomalous fluorescence, and this may also be inferred from the large scatter of points around the fitted line in, for example, the Lippert−Mataga plots. Also, other plots of this type are not showing a reasonable correlation between solvent-induced spectral shifts of the band F_A and solvent polarity.[8,10] The obvious reason for this is that the band F_A arises from a type of species (solute−solvent exciplex) which is different in each solvent.

There is no common opinion about the nature of the fluorescent states of BA. The band F_A of solutions of BA in nonpolar solvents is thought to arise from (1) a moderately polar excited bare BA molecule whose symmetry is neither[4,6] D_{2d} nor D_2, (2) a moderately polar excited twisted bare BA molecule (implying D_{2d} or D_2 symmetry),[9] (3) an excited bare BA molecule with D_{2d} symmetry and vanishing dipole moment,[8] (4) an excited bare BA molecule (implying D_{2d} or D_2 symmetry) with merely a solvent dependent effective torsional potential.[7] The band F_A of solutions of BA in polar solvents has been attributed to (5) solute−solvent exciplexes,[4] (6) an intramolecular charge transfer (TICT) excited state of a bare BA molecule with full electron transfer (presumably of the solute with D_2 symmetry),[8,10−14] (7) a moderately polar excited bare solute (presumably of the solute with D_2 symmetry).[15]

A structural modification of BA, which involves only a change of the twist angle of the two anthryl groups, causes the molecular symmetry to change from the ground state point group D_{2d} to the group D_2. The point groups D_{2d} and D_2 imply both a vanishing dipole moment.[1,4] Nevertheless, the discussions about the photophysics of BA are still strongly focused on the supposed relation between intramolecular charge transfer and twisting in the excited state.[15−18] It remains unclear how the solvent can assist in obtaining a polar state while D_2 symmetry is retained. Certain organic molecules with an electron donor and an acceptor in a delocalized system of electrons, such as, for example, dimethyl-aminobenzonitrile (DAMBN), are known to exhibit an anomalous dual fluorescence when they are dissolved in polar solvents. There is a preference in the literature to attribute this behavior to relaxation of the excited solute in polar solvents into a twisted intramolecular charge transfer (TICT)[19] state with complete charge separation and to assume that this applies also to solutions of BA.[8−15] This preference cannot be justified, because strong evidence has been provided that the anomalous fluorescence arises from the formation of 1:1 solute−solvent exciplexes.[19−24]

In the analysis of the dispersed fluorescence of BA in a supersonic molecular beam, a model is introduced that involves a double minimum potential for the torsional motion in the state S_1 in which the barrier is substantially displaced relative to the ground-state minimum.[16] The obtained potential for the torsional mode has been applied in the simulation of the fluorescence spectra of solutions of BA.[17,18] Theoretical and experimental objections can be raised against this model. If an electronic state of BA is found to be degenerate in a first-order description (e.g., spanning an irreducible representation E of D_{2d}), the application of a correction for vibronic coupling by a nontotally symmetric mode (Jahn−Teller coupling) may lead to a splitting. In contrast to the proposition, a single minimum results then in the potential for this mode in the upper electronic state, which is not displaced, while the potential for this mode in the lower electronic state is a double well with the minima displaced and the barrier coinciding with the minimum of the upper state. The experimental objection is that the model implies an extremely small radiative transition probability between the states S_1 and S_0 in contrast to the very large extinction coefficient in the first electronic absorption band,[1] the relatively large fluorescence quantum yield, and the mirror image relation[4] between the first electronic absorption band and the fluorescence band of a glassy solution at 77 K.

A more recent study[25] of the dispersed fluorescence of BA in a supersonic molecular beam reveals a regular spectrum with only sharp bands for the bare molecule, while this spectrum is strongly perturbed with additional broad features in the red part of the spectrum in the case of clusters of BA with either Ar or H_2O. The fluorescence of the clusters in the red spectral region is attributed to relaxation into a charge transfer state. A serious objection against this conclusion is that the isolated excited clusters cannot relax, because they are not coupled to a heat bath. The differences with the spectrum of bare BA may arise from the differences in the available amount of excess energy after excitation, from differences in the effects of internal redistribution of the excess energy, or from optical transitions leading to dissociation of the clusters in the electronic ground state. The latter possibility may also explain why the additional bands are very broad and without substructure.

Pump−probe type spectroscopic studies of solutions of BA have been reported. Some of these do not seem to agree with each other. Early work with nanosecond resolution revealed transient absorption bands of solutions of BA in acetonitrile differing in decay kinetics and arising from three different types of species.[4] One of them gives rise to a band at 690 nm with lifetime equal to the lifetime of the fluorescence. It has been attributed to the solute−solvent exciplex, because this band does not appear in the case of solutions in an alkane. Another species causes the appearance of a sharp band at 430 nm. Since its lifetime is longer than 50 μs, it has been charaterized as a BA molecule in a triplet state. The absorption spectrum of the third transient species persists at least 10 μs, exhibits second-order decay, and has intense bands at 425 and 730 nm and weaker bands in between. This spectrum has all the features of the UV/

visible absorption spectrum of the radical cation of anthracene and its quantum yield is proportional to the lifetime of the band F_A.[4] Therefore it has been attributed to a radical cation of BA emerging from the solute−solvent exciplex. Recently obtained transient absorption spectra of BA in butyronitrile at several temperatures fit nicely in this picture. The band around 690 nm can be seen clearly at 297 K. It decays while a new band is seen to grow between 730 and 800 nm at 165 K. Although this growing band has been attributed to an excited state of a bare BA molecule with full electron transfer, we take it as evidence for the formation of a radical cation that goes unnoticed at higher temperatures due to its participation in chemical reactions.[26] A number of studies led to the conclusion that a state with complete charge separation is not generated by photoexcitation of BA in polar solvents such as acetonitrile, because the transient absorption did not resemble a superposition of the spectra of the radical cation and anion of anthracene.[27,28] The opposite conclusion has been reached in a more recent study, although the reference spectra of the cation and anion on which this is based do not show the characteristic absorption around 700 nm.[8]

Not enough attention has been paid to the possibilities of symmetry breaking in the excited state of BA by complex formation with the solvent, by pyramidalization[4] of atoms C(9) and C(9′), or by exciplex formation provoked by pyramidalization of atoms C(9) and C(9′). Pyramidalization is realized in the photodimer of anthracene with bonds between the atoms in the pairs C(9), C(9′) and C(10), C(10′).[29−32] If the bond between atoms C(10) and C(10′) in the photodimer is broken, while C(9), C(9′) are dehydrogenated, one obtains a structure that might be obtained by photoexcitation of BA. This structure or a metastable intermediate on this reaction path could be involved in the multiple fluorescence of BA in alkanes when they are formed adiabatically from the primary excited state. Note that a large deviation from planarity may appear in an electronically excited aromatic ring system. This has been observed in the case of pyridine in its lowest triplet state.[33] All these mechanisms imply modification of the fluorescence spectrum and dependence of the excited-state dynamics on solvent viscosity. It seems that preoccupation with TICT has led the search for a proper explanation of the fluorescence behavior of BA in a wrong direction.

Here we report a study of solutions of BA in the nonpolar solvents cyclohexane and 1,4-dioxane and in the polar solvent propionitrile by means of polarization selective time-resolved spectroscopy. Attention is paid to the kinetics of depolarization of the photoinduced transient absorption and fluorescence and to the kinetics of excited-state populations. The depolarization kinetics of excited BA and anthracene in cyclohexane and in 1,4-dioxane are compared to see whether excited-state solute−solvent complexes are involved. Relevant theoretical aspects of depolarization of optical transitions through rotational diffusion are presented. The excited solute is treated as an ellipsoid subjected to slip boundary conditions.

Experimental Section

The laser system used in the pump−probe studies has been described previously.[34] It consists of a c.w. mode locked titanium saphire oscillator followed by a 1 kHz regenerative amplifier yielding amplified pulses of about 900 μJ, 200 fs at either 790 or 794 nm. This system has been used in three different setups. The first two were designed to study the time dependence of photoinduced transient UV/visible absorptions. The third one served to study the time dependence of the fluorescence.

In the first setup, optical pulses generated as the second harmonic of the amplified laser pulses (395 nm) were used in a frequency conversion process in a system consisting of an optical parametric generator (OPG) and amplifier (OPA) to get pump pulses for the primary excitation of the sample. They had a total energy per pulse (E_P) of about 3 μJ and were tunable in wavelength between 350 and 385 nm. Some of the residual energy of the 395 nm pulses emerging from the OPA/OPG system was used to probe the evolution of the excited sample. The beam for pumping the sample was split into a reference pump beam, used to monitor E_P, and an actual pump beam. The beam for probing was also split to obtain a reference probe beam and an actual probe beam. The former passed the sample through a region outside the excited volume, whereas the latter went through the excited volume. In this configuration the wavelength of the pump pulse was tuned to match the maximum in the first UV absorption band of the solute (either anthracene or 9,9′-bianthryl).

In the second setup the laser system generated 397 nm pulses in a beam which was split to pump the sample with one fraction of the pulse energy and to generate probe pulses with the other fraction in the OPG/OPA system. The probe pulses were now tunable in wavelength between 450 and 807 nm.

In the third setup the 794 nm beam from the laser oscillator was split to provide a probing beam and an input beam for the amplifier. The second harmonics of the amplified pulses (397 nm) were used to pump the sample, and the emerging fluorescence was collected with an achromatic lens and upconverted in frequency by mixing with the probing light in a optically nonlinear crystal (BBO, 0.1 mm). The resulting pulse at the sum frequency was then filtered by a monochromator, detected with a photomultiplier (Hamamatsu R1463P) and recorded with a gated photon counter (Becker and Hickl PHC-322) equipped with both a signal and reference input channel. The reference signal for the photon counter was generated in a separate BBO crystal by sum frequency generation of two reference beams, obtained by splitting the pump and probe beams. A normalized fluorescence was calculated as the ratio of the magnitudes of the signal and reference outputs of the photon counter. The influence of laser intensity fluctuations on the normalized fluorescence intensity was eliminated in this manner.

The sample was contained in a cylindrical cell of 1 mm path length and 50 mm diameter rotating at high speed around its axis. Pump and probe beams entered the sample cell perpendicular to its windows and were collinear and off axis with respect to the cylinder axis. In this manner effects of sample decomposition could be avoided, because each pump−probe pulse pair investigated a fresh portion of the sample. The induced change in optical absorbance, $\Delta A(\lambda,t)$, was determined from the attenuation of each probe pulse transmitted through the sample. The time (t) elapsed between primary excitation and probing was varied by means of an optical delay line. In this manner the absorbance change at fixed wavelength (λ) is obtained as a function of time, $\Delta A_\lambda(t)$. The value of $\Delta A_\lambda(t)$ at fixed t was averaged over sufficiently long times to achieve a good signal-to-noise ratio. To compare changes in absorbance at different wavelengths, $\Delta A_\lambda(t)$ was normalized with respect to E_P. The optical alignment of pump, probe, and reference beams was kept fixed in a series of recordings that were compared, and it was verified that E_P remained constant while t was scanned. An indication of spectral changes with time was obtained by plotting $\Delta A_t(\lambda)$, which represents $\Delta A(\lambda,t)$ at the discrete λ's for various specified times. The angle of the polarization of the probe beam with respect to that of the pump beam was changed by means of an appropriate $\lambda/2$ plate.

Measurements were performed for a probe beam with perpendicular and parallel polarization as well as for magic angle (54.7°). Note that the spectral resolution in the experiments is too low to resolve kinetic differences among the members of the inhomogeneous ensemble of observed molecules.

The recorded time dependent signals for parallel and perpendicular polarizations of the probe beam were used to calculate the anisotropy, provided the signal-to-noise ratio was sufficiently large. When these signals were rather noisy, they were first represented by a fitted (multiexponential) function prior to the calculation.

The cross correlation function of the pump and probe pulse has been determined both in the case of the first and the second configuration by determining the time profile of the two-color two-photon absorption of the solvent 1,4-dioxane.[34] The width of the cross correlation function was always less than 450 fs, and this has been considered as the instrumental response time in the pump−probe experiments.

The normalized fluorescence intensity was measured for different wavelengths by appropriate tuning of the angle of the BBO crystal, in which fluorescence and probe beam were mixed. The probe beam was delayed with an optical delay line to measure the time dependence of the emitted fluorescence. The angle of polarization of the pump beam was varied by means of a $\lambda/2$ plate to determine the fluorescence intensity for parallel and perpendicular polarization and for magic angle. The anisotropy of the fluorescence (r_F) was calculated from the normalized intensities for parallel and perpendicular polarization.

All measurements have been performed at room temperature, $T = 295$ K.

9,9′-Bianthryl was recrystalized from a solution in acetic acid anhydride and then dried in a vacuum over KOH pellets. The solvent propionitrile (PN, Janssen) of analytical grade was distilled over P_2O_5 prior to use. Spectroscopic grade cyclohexane (CHX, Merck) was used as received. Before the solvent 1,4-dioxane was used, sodium was added to it and then it was boiled in a refluxing apparatus for several hours and distilled subsequently. None of the solvents used showed any (linear) absorption in the UV and visible wavelength range covered. The solutions were not deoxygenated, and their absorption spectra were recorded on a Perkin-Elmer Lambda 2 UV−vis spectrophotometer. The concentration of the solutions of BA in CHX and BA in PN was smaller than 5×10^{-4} mol/L, which corresponds to a maximum optical density of 0.5 at 385 nm. The absorption spectra of the solutions before and after their use in the pump−probe studies were compared, and no change was observed.

Theoretical Treatment of Depolarization of Optical Transitions. Time- and polarization-resolved pump−probe spectroscopy and fluorescence depolarization as a function of time are suitable methods to study the rotational Brownian motion of excited solute molecules in liquid solutions. Let *x*,*y*,*z* represent the orthonormal system of axes in the solute, for which the rotational diffusion tensor **D** is diagonal. In this system **u** and **v** are unit vectors directed along the transition moment for the pump and the probe transition, respectively. Their Cartesian coordinates in the molecular frame are (u_x,u_y,u_z) and (v_x,v_y,v_z). The angle between the *z*-axis and **u** and between the *z*-axis and **v** are θ_u and θ_v, respectively, while the projections of **u** and **v** on the *x*,*y*-plane make angles φ_u and φ_v with the *x*-axis, respectively. The sample is pumped by a short polarized light pulse and probed subsequently by absorbed or emitted light. Let I_P and I_S represent either the probed absorbance or fluorescence intensity for polarization parallel (P) or perpendicular (S) to the polarization of the pump beam, respectively. The probed anisotropy *r* is defined as

$$r(t) \equiv \frac{I_P(t) - I_S(t)}{I_P(t) + 2I_S(t)} \tag{1}$$

When the depolarization is caused only by rotational Brownian motion of the solute, $I_P(t)$ and $I_S(t)$ may be written as[35]

$$I_P(t) = \frac{1}{9} C(t) + C(t) \sum_{j=1}^{5} \Omega_j \exp(-\gamma_j t) \tag{2}$$

where the expressions for the Ω_j and γ_j terms can be found in the literature,[35] but are given for the sake of convenience in the appendix. In the case where both the pump and probe processes involve single electronic transitions, the anisotropy will be written as

$$r(t) = \sum_{j=1}^{5} \Phi_j \exp(-\gamma_j t) \tag{3}$$

where the coefficients Φ_j are given by equations A18−A22 in the appendix. Note that the quantity $Q_j = \gamma_j \Phi_j$ is a measure of the weight of the *j*th term in the expansion of $r(t)$.

Special attention is needed for the case in which the probe process involves a single electronic transition, but the pump process involves two electronic transitions with probabilities f_1 and f_2. The signal I_P consists then of contributions I_{P1} and I_{P2}, arising from the first and second electronic transition in the pump process, respectively. Similarly I_S consists of contributions I_{S1} and I_{S2}. Then $r(t)$ is given by

$$r(t) = \frac{(I_{P1} + I_{P2}) - (I_{S1} + I_{S2})}{(I_{P1} + I_{P2}) + 2(I_{S1} + I_{S2})} \tag{4}$$

from which one may derive the expression

$$r(t) = \frac{1}{1 + p} \sum_{j=1}^{5} (\Phi_{1j} + p\Phi_{2j}) \exp(-\gamma_j t) \tag{5}$$

in which the coefficients Φ_{1j} and Φ_{2j} are given in the equations A25−A29 in the appendix.

The solute will be represented as an asymmetrical ellipsoidal body. Taking the longest semi-axis in the *x* direction and its length as the unit of length, the ellipsoid is described by

$$x^2 + \frac{y^2}{a} + \frac{z^2}{b} = 1 \tag{6}$$

where *a* and *b* are the lengths of the short semi-axes.

The Stokes−Einstein−Debye (SED) hydrodynamic treatment of the rotational diffusion of solute molecules in liquid solutions has often been shown to be adequate.[36] Reference 36 provides access to a list of other relevant publications. In the SED theory, the frictional torque on the solute is depending on the molecular geometry of the solute, on the temperature (T) and viscosity (η) of the solvent, and on the boundary condition. Either stick or slip hydrodynamic boundary conditions have been used to obtain expressions for the rotational relaxation time τ_R of the solute. Since the friction arises from the displacement of solvent molecules, it depends implicitly only on solvent−solvent molecular interactions. The choice of boundary conditions can therefore not be based on considerations of solute−solvent molecular interactions. This means that the stick condition is

not necessarily more appropriate than the slip condition in the treatment of a polar solute in a polar solvent. The stick boundary condition has been shown to be inadequate on several occasions.[37,38] By imposing the stick boundary condition, the calculated rotational relaxation times are much larger than the corresponding experimental values. An examination of rotational relaxation times of solutes in a wide variety of solvents has shown that the slip boundary condition is adequate for solutes with molecular volumes up to 1000 Å.[39] Another reason to favor the slip condition is that the rotational relaxation time of practically spherical solutes such as adamantane and campher is cited to be independent of viscosity.[38] This result cannot be reproduced with the stick condition. Based on the considerations above, slip boundary conditions will be used here.

The time constant τ_R has been suggested[38] to satisfy the following empirical relation between the experimentally determined rotational diffusion time τ_{xp} and the effective free rotational diffusion time τ_0:

$$\tau_{xp} = \tau R + \tau_0 \tag{7}$$

where

$$\tau_0 = (2\pi/9)\sqrt{\frac{I}{k_B T}} \tag{8}$$

and I is the average moment of inertia. This relation has been found to agree with experiment in a number of cases where the time dependent optical anisotropy $r(t)$ is a single exponentially decaying function of t.[36,38,40] Note that a nonvanishing and positive value of τ_0 makes sense, because rotational diffusion of the solute should persist at $\eta = 0$. However, application of eq 7 yielded negative values of τ_0 in certain experiments.[36] The obvious reason for this is that the experimental values τ_{xp} were obtained by transformation of spectral line shapes, without consideration of inhomogeneous broadening and other possible sources of spectral broadening. An incomplete theoretical treatment[41] yielded also a negative value of τ_0. This theory is obviously not reliable, because a negative relaxation time will not be encountered in the real world.

The rotational friction coefficients ξ_x, ξ_y, ξ_z for an ellipsoidal body under slip boundary condition have been derived in ref 42, and a revised numerical evaluation of those results is tabulated in ref 43 for a series of values of a and b. The friction coefficients for intermediate values of a and b can be obtained from the table by applying a bicubic method of interpolation. The diffusion coefficients are related to the solvent's viscosity η, the molecular volume V, and the listed friction coefficients in the following manner:

$$D_j = \frac{k_B T}{\eta V \xi_j} \quad with\ j = x, y, z \tag{9}$$

where k_B is Boltzmann's constant and T is the temperature of the sample. The table of friction coefficients and the procedure for bicubic interpolation are used in a computer program which generates the function $r(t)$ for the given values of η and T as a function of a, b, V, the orientation of the pump and probe transition moments, and the factor p in the case of overlapping bands at the pump wavelength. By variation of these parameters, an accurate fit can be obtained between the generated and the experimental $r(t)$. The parameter p affects only the value of $r(0)$.

When the pump and probe processes involve each single electronic transition, the initial anisotropy of the probe signal is limited to the range $-0.2 \le r(0) \le 0.4$. The lower and upper limits correspond respectively to mutual perpendicular and mutual parallel polarization of the transitions in the pump and probe processes. However, when stimulated emission is also affecting the magnitude of the probe signal, the value of $r(0)$ may be far beyond these limits. This can be seen by considering the probe process as involving, for example, a single transient absorption process and a single stimulated emission process. The effect of the superposition may be expressed as

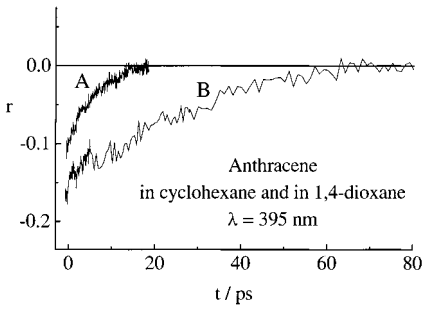

Figure 1. Decay of the anisotropy of the transient absorption of anthracene in cyclohexane (upper curve, A) and in 1,4-dioxane (lower curve, B) at a probe wavelength of 395 nm.

$$r = \frac{r_j\{I_P(j) + 2I_S(j)\} + r_k\{I_P(k) + 2I_S(k)\}}{I(j) + I(k)} \tag{10}$$

with

$$I(n) \equiv I_P(n) + 2I_S(n) \quad for\ n = j,k \tag{11}$$

Two numerical examples will illustrate the effect of the contribution of the stimulated emission. In the first one we take $I(j) = 1$; $r_j = -0.2$ with $I(k) = -0.2$; $r_k = 0.4$ and obtain $r = -0.35$ and in the second one we take $I(j) = 1$; $r_j = 0.4$ with $I(k) = -0.2$; $r_k = -0.2$ and obtain $r = 0.55$.

Results and Discussion

1. The Solute Anthracene. The function $r(t)$ has been determined experimentally with a time resolution of 0.2 ps by detecting the transient absorption and the stimulated emission (negative transient absorption) of anthracene in its lowest excited electronic singlet state (S_1), generated by photoexcitation of a solution in cyclohexane or in 1,4-dioxane, Figure 1. This experimental function will be denoted as $r_A(t)$. The experimental function of the fluorescence anisotropy, presented later on, will be denoted in the same way as $r_F(t)$. It is a monoexponentially decaying function given by

$$r_A(t) = r_A(0)\exp\left(-\frac{t}{\tau_A}\right)$$

The solution in cyclohexane ($T = 295$ K; $\eta = 0.94$ cP) yielded $r_A(0) = -0.12$ and $\tau_A = 5.9$ ps, whereas $r_A(0) = -0.18$ and $\tau_A = 27.4$ ps were obtained in the case of the solution in 1,4-dioxane ($T = 295$ K; $\eta = 1.2$ cP). The sign and magnitude of $r_A(0)$ will be discussed later on.

The function $r(t)$ for anthracene in the S_1 state had been determined previously[44,45] with much less accuracy by single photon counting of the fluorescence. Monoexponential decay had been observed with a time constant of 6.3 ps when $\eta = 1$ cP (solvent: liquid paraffin)[44] or 8 ps when $\eta = 1$ cP (solvent: cyclohexane).[45] In the case of the fluorescence, the initial value of r_F, i.e. at time $t = 0$, amounts to $r_F(0) = 0.198$. This value was determined by using a solution in a highly viscous solvent.[45] It seems quite certain that rotational motion of the solute during

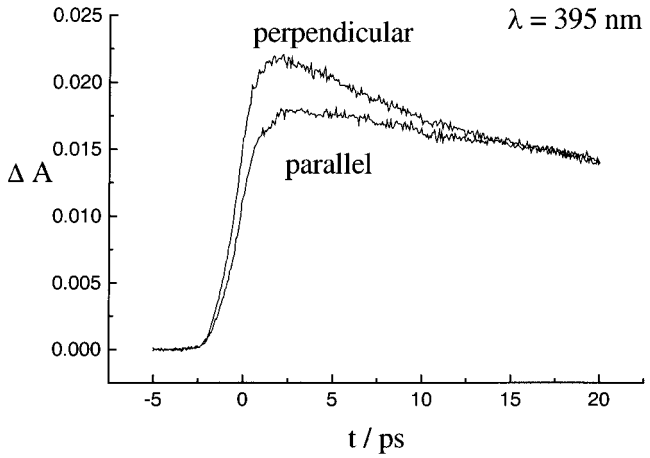

Figure 2. Transient absorbance $\Delta A_i(t)$ of anthracene in cyclohexane at 395 nm for both parallel (lower curve) and perpendicular (upper curve) polarization of the probe beam.

the pump pulse has been inhibted in this manner. The rotational diffusion of anthracene in the electronic ground state (S_0) has been studied by detecting the time integrated fluorescence generated by vibrational excitation followed by a time delayed UV excitation.[37] The obtained function $r_F(t)$ for anthracene in the state S_0 is decaying monoexponentially with a time constant of 19 ps for a solution in CCl_4 at 294 K (with $\eta = 0.97$ cP) and 13 ± 2 ps for a solution in perdeuteriobenzene at 294 K.[37] The ratio I_P/I_S of the magnitudes of the signals observed with parallel and perpendicular polarization of the second pulse amounting to 1.7 and 1.8 for the solution in CCl_4 and perdeuteriobenzene, respectively. This amounts to $r_F(0) = 0.19$ in the case of the solvent CCl_4 and $r_F(0) = 0.21$ in the case of perdeuteriobenzene. These values are much smaller than expected when the transition moments of the two sequential transitions are mutually parallel. This observation has been attributed to partial decay of the anisotropy, which could result from rotational motion of the solute in the course of the pumping process. However, this explanation is contradicted by the fact that the larger value of $r(0)$ is obtained for the fastest decaying anisotropy (perdeuteriobenzene).

It is often assumed that the first UV absorption band of anthracene is covering a single electronic transition and that the transition moment lies along the short axis in the molecular plane.[37,44,45] Then both the fluorescence anisotropy and the anisotropy in the two-step excitation process should yield an initial value $r_F(0) = 0.4$, in contrast to the observations. An explanation for the value $r_F(0) = 0.2$, which applies to both types of experiment is that the first UV absorption band of anthracene is covering two electronic transitions with mutually perpendicular in-plane transition moments. The strongest UV pump transition is taken to be polarized along the short axis (i.e. the *y*-axis in the notation here). The coefficients Φ_{1j} and Φ_{2j} (eq 5) can only be nonvanishing for $j = 1$ and $j = 2$. Since the function $r(t)$ is then in general a biexponentially decaying function of *t*, the observed monoexponential behavior must arise from the special ellipsoidal shape of anthracene. The observed value $\tau_A = 5.9$ ps is not very different from the values 6.3 and 8 ps, resulting from the decay of the fluorescence anisotropy. In contrast to the value $r_F(0) = 0.2$, obtained in the case of the fluorescence of the solution in cyclohexane, the transient absorption measurement yields $r_A(0) = -0.12$. To understand the difference between these two values of $r_{xp}(0)$, one has to consider the magnitude of the transient absorption relative to the contribution from stimulated emission. Figure 2 shows that the absorbance is positive for both parallel and perpendicular polarization of the probe beam. This means that the absorbance arises predominantly from transient absorption. The negative sign then indicates a main contribution from a transient absorption polarized along the long in-plane axis. Unfortunately, the contribution of the stimulated emission to the negative value $r_A(0) = -0.12$ cannot be estimated and therefore we have to resort to the value $r_F(0) = 0.2$, found in the case of the fluorescence anisotropy, in the optimization process of the geometrical parameters.

The transient absorption measurements of the solution of anthracene in 1,4-dioxane yield a value of τ_A that is nearly four times larger than in the case of the solution in cyclohexane. This is evidence that in the solution in 1,4-dioxane, the anthracene in the state S_1, is observed in the form of a solute−solvent complex. The positive sign of the absorbance for both parallel and perpendicular polarization in the dioxane case together with the negative value $r_A(0) = -0.18$ indicate again the contribution of a transient polarized perpendicular to the polarization of the ground-state absorption.

The viscosity-dependent part of the induced anisotropy of anthracene will be described as $r(t) = r(0)\exp(-t/\tau_R)$ with τ_R the viscosity-dependent time constant and given in ps. The calculated value of τ_0 amounts to $\tau_0 = 1.3$ ps for anthracene in the state S_0. The experimental value of τ_0 can be estimated graphically from the plot in Figure 5 of ref. 37, using the data points for solutions of anthracene in perdeuteriobenzene, CCl_4 and C_2Cl_4. This amounts to $\tau_0 = 1.2$ ps. Because this does not differ significantly from the theoretical estimate, the latter will be used here for both the state S_0 and the state S_1. The parameters *a*, *b*, *V*, *p* for anthracene in both the state S_1 and S_0 have been optimized around two values of the volume, $V = 165$ and $V = 220$ Å^3, to obtain a calculated function $r(t)$ that reproduces the experimental function $r_0\exp(-t/\tau_R)$. The volume $V = 165$ Å^3 is obtained by adding the van der Waals increments of the atoms in anthracene,[8] and the volume $V = 220$ Å^3 has been quoted as the result of a simulation.[45] The values of *a* and *b* have a strong effect on the relative contributions of the two components in the biexponential decay of $r(t)$. The factor *p* has mainly an influence on the magnitude of $r(0)$. The volume *V* has a strong effect in scaling of the time constant to the required magnitude. The actual lengths of the semi-axes in the *x*, *y*, and *z* directions of the optimized ellipsoid for anthracene in the state S_1 in cyclohexane with $V = 165$ Å^3 (columns 4 and 5 in Table 1) are $A = 5.11$, $B = 3.52$, $C = 2.19$ Å, respectively. For anthracene in CCl_4 in the state S_0, the optimized parameters correspond to $A = 6.96$, $B = 3.69$, $C = 1.53$ Å, when $V = 165$ Å^3. The latter two results indicate that the large difference in the time constants for the rotational diffusion of anthracene in the states S_0 and S_1 is arising from a difference in molecular shape.

If one assumes that excited anthracene exists also as a bare solute in the solution in 1,4-dioxane, then the geometrical parameters obtained above should be suitable to simulate the depolarization dynamics also in this case. With this set of parameters agreement with experiment (second column in Table 2) can be obtained, provided that the viscosity of 1,4-dioxane at 295 K is assigned the unrealistic value of 5.45 cP, instead of the true value of 1.2 cP. The conclusion emerging from this is that excited anthracene in 1,4-dioxane does not exist in the form encountered in the solution in cyclohexane. To get agreement in this case with experiment, when the value of the viscosity is set at 1.2 cP, the volume has to be increased considerably beyond the value of 165 Å^3 for the bare solute. This is evidence

TABLE 1: Geometrical Parameters of Anthracene

state	S_1				S_0			
solvent	CHX				CCl_4			
τ_{xp}/ps	5.9 ± 0.1	5.9 ± 0.1	5.9 ± 0.1	5.9 ± 0.1	19 ± 2	19 ± 2	19 ± 2	19 ± 2
r (0)	0.4	0.2	0.4	0.2	0.4	0.2	0.4	0.2
p	0	0.5	0	0.5	0	0.5	0	0.5
τ_0/ps	1.3	1.3	1.3	1.3	1.3	1.3	1.3	1.3
Φ_1	0.4	0.2	0.4	0.2	0.4	0.2	0.4	0.2
γ_1/ps	4.6	4.6	4.6	4.6	17.9	17.9	17.9	17.9
Φ_2	0	0	0	0	0	0	0	0
γ_2/ps	9.2	9.2	9.2	9.2	35.6	35.6	35.6	35.6
a	0.72	0.72	0.6875	0.6875	0.57	0.57	0.53	0.53
b	0.48	0.48	0.4277	0.4277	0.26	0.26	0.22	0.22
V/[Å^3]	220	220	165	165	220	220	165	165
A/[Å]	5.33	5.33	5.11	5.11	7.08	7.08	6.96	6.96
B/[Å]	3.84	3.84	3.52	3.52	4.04	4.04	3.96	3.96
C/[Å]	2.56	2.56	2.19	2.19	1.84	1.84	1.53	1.53

TABLE 2: Geometrical Parameters of Solute−Solvent Exciplexes in the Solution of Anthracene in 1,4-Dioxane

	state S_1				
	bare solute	1:2 exciplex	1:1 exciplex	1:1 exciplex	1:1 exciplex
τ_{xp}/ps	27.4 ± 0.1	27.4 ± 0.1	27.4 ± 0.1	27.4 ± 0.1	27.4 ± 0.1
main absorption	*y*-polarized	*x*-polarized	*y*-polarized	*x*-polarized	*x*-polarized
r (0)	0.20	0.20	0.20	0.20	0.20
η/cP	5.33	1.20	1.20	1.20	1.20
p	0.50	0.50	0.50	0.50	0.50
τ_0/ps	1.30	2.50	2.10	2.10	2.10
Φ_1	0.20	0.10	0.20	0.00	0.00
γ_1/ps	26.10	0.86	25.30	0.02	12.74
Φ_2	0.00	0.10	0.00	0.20	0.20
γ_2/ps	52.20	24.90	50.40	25.30	25.31
a	0.69	0.93	0.56	0.52	0.65
b	0.43	0.50	0.26	0.50	0.37
V/[Å^3]	165.00	326.00	245.50	245.50	245.50
A/[Å]	5.11	5.51	7.38	6.08	6.28
B/[Å]	3.52	5.13	4.16	3.17	4.06
C/[Å]	2.19	2.76	1.91	3.05	2.30

that anthracene in its state S_1 exists in 1,4-dioxane as a solute−solvent exciplex. Taking the specific shape of 1,4-dioxane into account, the rotational diffusion tensor of such an exciplex is not expected to be diagonal in the system of molecular axes *x*, *y*, *z* in the solute as assumed in the simulation of the kinetics of depolarization. Pronounced multiexponential decay of $r(t)$ is then to be expected, in contrast to our observation. We assume therefore that the solute−solvent exciplex has a special structure with the axes *x*, *y* (directions of transition moments) in the solute nearly coincident with a principal axes of the rotational diffusion tensor. This situation could arise when the excited solute is present as a 1:2 solute−solvent exciplex and is less likely to be encountered in the case of a 1:1 solute−solvent exciplex. The volume of the exciplex has to be approximately equal to the volume of excited anthracene with the van der Waals volume of 1,4-dioxane added twice or once. The third column of Table 2 list the geometrical parameters of the 1:2 exciplex, which yield satisfactory agreement between simulated depolarization kinetics and experiment, when the volume is fixed at 326 Å^3. The simulated depolarization kinetics is biexponential, but its fast component is too insignificant to be observable.

2. The Solute 9,9′-Bianthryl. *2a. Solution in Cyclohexane.* The time dependence of the anisotropy $r_F(t)$ of the fluorescence and of the transient absorption from the S_1 state of BA in cyclohexane has been recorded. The achieved signal-to-noise ratio is much better in the latter case than in the former case. The anisotropy $r(t)$ exhibits monoexponential decay in both cases. The transient absorption yields a time constant for $r_A(t)$ which amounts to $\tau_A = 49 \pm 1$ ps, independent of the probe wavelength. An example is given in Figure 3 that shows the anisotropy decay of the transient absorption at a probe wavelength of 575 nm. The fluorescence yields $\tau_F = 52 \pm 5$ ps as the time constant for $r_F(t)$ (Figure 4). The more accurate value $\tau_A = 49 \pm 1$ ps will therefore be considered to apply also in the case of the fluorescence. Although τ_F is wavelength independent, the initial value of $r_F(t)$ is not constant over the whole wavelength region covered. This indicates that several transitions with various directions of the transition moments are encountered.

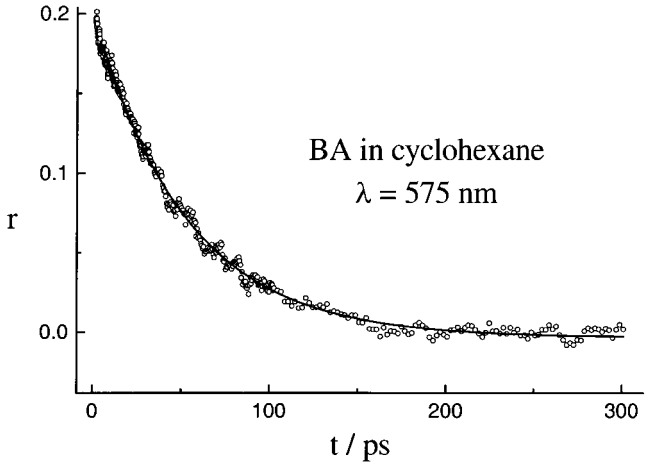

Figure 3. Monoexponential decay of the anisotropy of the transient absorption of BA in cyclohexane probed at 575 nm. The line through the data points represents the fitted function.

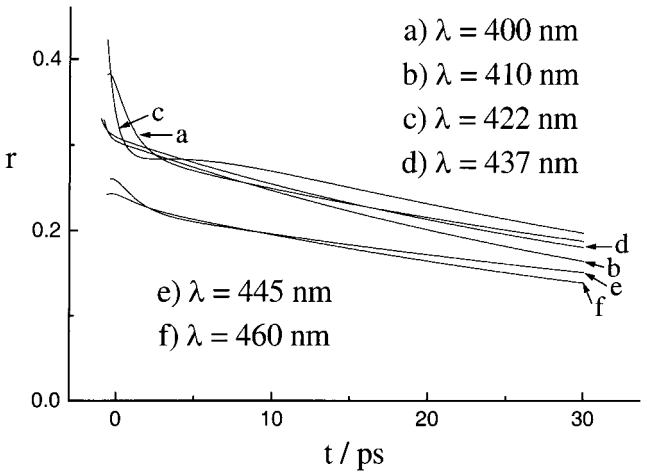

Figure 4. Variation of the initial value of the anisotropy of the fluorescence of BA in cyclohexane at various wavelengths (upper group: 400, 410, 422, 437 nm; lower group: 445, 460 nm).

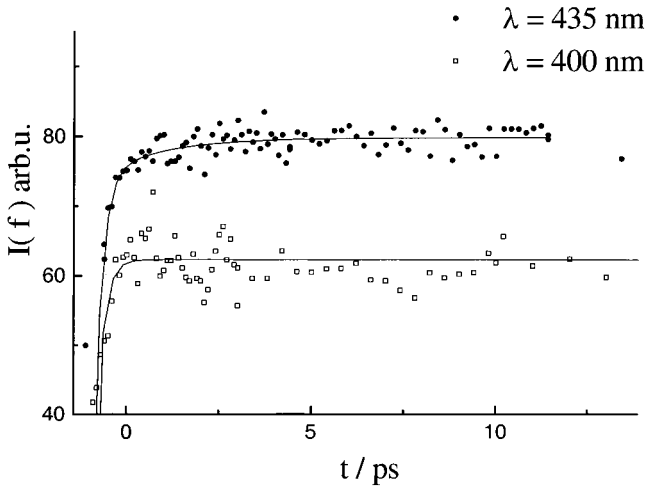

Figure 5. Time dependence of the fluorescence intensity (magic angle) of BA in cyclohexane at 400 nm (lower curve) and 435 nm (upper curve with small growth component).

The fluorescence (Figure 4) yields an initial value $r_F(0) \approx 0.4$ at 400, 410, 422, and 437 nm. The value $r(0) = 0.4$ is characteristic for single electronic transitions in both the pump and the probe processes with their transition moments mutually parallel. This means that the emission in the region $400 \leq \lambda \leq 437$ nm is normal fluorescence (F_N) emitted by bare excited 9,9′-bianthryl molecules (N^*). The value $r(0) = 0.4$ means also that interaction of the two anthryl groups has caused a significant separation of the two transitions under the envelope of the first UV absorption band of anthracene. Note that the fluorescence quantum yield (Φ_f) increases from $\Phi_f = 0.36$ for anthracene in cyclohexane[46] to $\Phi_f = 0.55$ for BA in cyclohexane.[9] This difference suggests that the S_1 state of BA is not merely a weakly perturbed S_1 state of anthracene. The transition moment of the $S_0 \rightarrow S_1$ transition of the BA molecules with fluorescence in the region $400 \leq \lambda \leq 437$ nm must be directed along the C(9)−C(9′) line, while the atoms C(10), C(10′), C(9), and C(9′) are collinear.

The fluorescence of BA in cyclohexane at 445 and 460 nm yields smaller initial values of $r_F(t)$. These are in the range $0.3 \leq r(0) \leq 0.4$ and indicate that fluorescence bands of different excited species are overlapping at these wavelengths. This conclusion is supported by the time dependence of the fluorescence of the solution, observed with polarization at magic angle (Figure 5), which shows a small growth component at 435 nm that does not appear at 400 nm. The variations in $r(0)$ just mentioned are not likely to arise from vibronic coupling of a single electronic state, because this does not introduce a time dependence in the spectrum, in contrast to our observation. A previous study[4] led also to the conclusion that the fluorescence of BA in cyclohexane is emerging from various types of species.

The simulation of the decay of the anisotropy of the fluorescence of BA in cyclohexane in the region $400 \leq \lambda \leq 437$ nm is rather straightforward. We adhere to the slip boundary condition which proved suitable in the case of anthracene. This implies an extremely short rotational relaxation time for the ground state geometry of BA with all three semi-axes of the ellipsoid of nearly equal length. Representing the ground-state molecule by a sphere, one gets a vanishing rotational relaxation time. The observed time constant of 49 ps for the fluorescence depolarization means that a representation by a sphere is not adequate for the excited molecule. Therefore, the excited molecule will be represented by an ellipsoid with a volume twice as large as the volume obtained for anthracene, i.e. $V = 330$ Å^3. The estimated free rotation relaxation time amounts to $\tau_{p0} = 2.4$ ps.

TABLE 3: Simulation of Fluorescence Depolarization Kinetics for 9,9′-Bianthryl in Cyclohexane Taking Transition Moments along C(9)−C(9′)

τ_{xp}/[ps]	τ_0/[ps]	τ_R/[ps]	$r(0)$	V/[Å^3]	a	b
49 ± 1	2.4	46.6	0.4	330	0.472	0.3655
Φ_1	γ_1/ps	Φ_2	γ_2/ps	A/[Å]	B/[Å]	C/[Å]
0	3.7	0.4	46.6	7.7	3.63	2.81

Table 3 shows that a biexponential decay of the anisotropy of the fluorescence is obtained in the simulation with a component having a time constant $\gamma_1 = 3.7$ ps, which is too insignificant to be observable. The major component in the simulation matches the experimental result. The obtained geometrical parameters yield semi-axes of the ellipsoid $A = 7.7$ Å; $B = 3.63$ Å; $C = 2.81$ Å. This is a geometry that differs significantly from that of the ground state, which is expected to have A ≈ B ≈ C (i.e. nearly spherical) and consequently vanishingly small rotational relaxation time under slip condition. The structural change in the excited state must be such that the direction of the transition moment is kept fixed in space, because this process would otherwise cause rapid depolarization, in contrast to observation. Such a structural change will be described after some other important facts have been presented first.

The features of the transient absorbance of BA in cyclohexane at 520 nm (Figure 6) provide an indication for the appearance of a species on a picosecond time scale. Note in this figure that a growth component is observed under magic angle polarization which does not appear in the evolution of the anisotropy. The time constant of the growth component amounts to 9.8 ps. A growth component with time constant of 9.8 ps could be observed also in the transient absorbance at 395 nm. This is shown in Figure 7. To the left of the dashed vertical line in this figure the signals for the parallel, magic angle, and orthogonal polarization increase fast and follow the pump pulse instantaneously. The signal at magic angle is positive in the early stage, and this means that the transient absorption exceeds then the stimulated emission intensity. This signal becomes negative after less than 5 ps, and this means that the gradually growing stimulated emission becomes then dominant. Note that rotational diffusion does not contribute to the time dependence of the

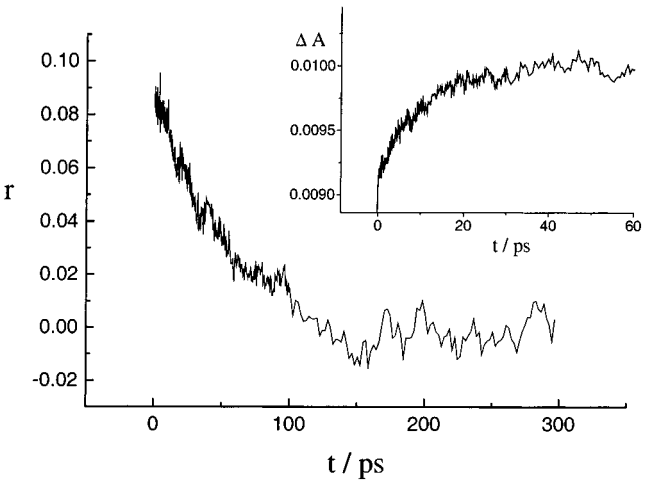

Figure 6. Monoexponential decay of the anisotropy of the transient absorption at 520 nm (main display) and monoexponential growth of the transient absorption at the same wavelength, but observed with magic angle polarization (inset), in the case of a solution of BA in cyclohexane.

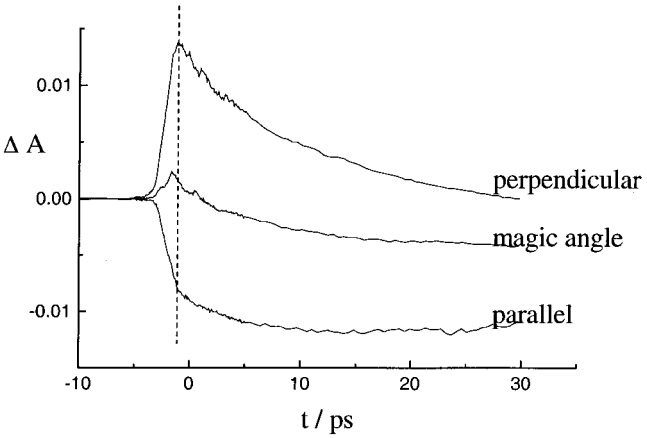

Figure 7. Transient absorbance $\Delta A_x(t)$ of BA in cyclohexane at 395 nm when the probe beam is polarized either parallel or perpendicular or at magic angle with respect to the polarization of the pump beam.

signal observed with magic angle polarization. Its evolution may arise from the time dependence of either the excited population or the excited-state transition probability. Nonspecific solute−solvent interactions could modify the transition probability, but this may be disregarded in the present case, because the response of the excited solute to the interaction with cyclohexane (dominated by its electronic polarizability) should be practically instantaneous compared to the time constant of 9.8 ps. Therefore the growth of the stimulated emission indicates that the excited-state species is being converted into one with a less strong absorbance. These conclusions agree with the picture containing three different fluorescing species of BA in alkanes, which emerged from a previous study.[4] The primary excited state of BA (S_{F1}) was found to be converted by thermal activation into two secondary fluorescent species (S_{F2} and S_{F3}) which get into thermal equilibrium within less than 100 ps. Taking these findings into account, the growth component at 520 nm with time constant of 9.8 ps is attributed to the conversion of species in state S_{F1} into interconverting species in the states S_{F2} and S_{F3}. Apparently these processes do not lead to depolarization of the observed fluorescence and transient absorption. Obviously, the geometry in the state S_{F1} must be the same as in the ground state and therefore the dipole moment must vanish also in the state S_{F1}. The previously observed transient dielectric loss

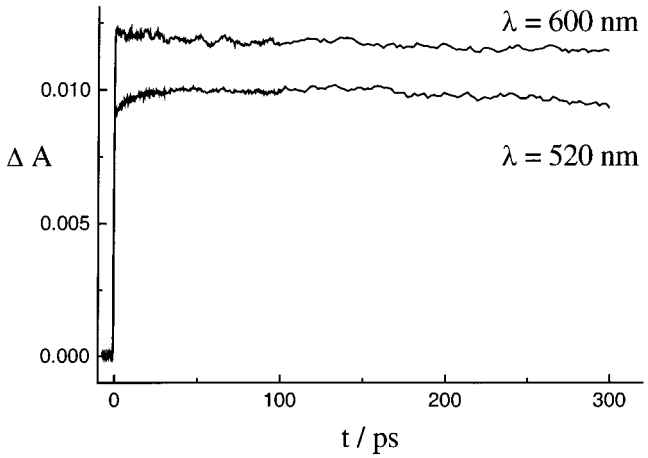

Figure 8. Long time behavior of the transient absorbance for probe light polarized at magic angle at 520 and 600 nm in the case of BA in cyclohexane.

must therefore be attributed to species in the states S_{F2} and S_{F3}. In other words, at least one of the latter species must have a nonvanishing permanent dipole moment. To describe a structure that may emerge with the direction of the transition unchanged and also with a permanent dipole moment, we will refer by group 1 and group 2 to the anthryl group containing atoms C(9), C(10) and C(9′), C(10′), respectively. We suggest that the difference in the electron distribution between the ground state and the excited state of the structures corresponding to the states S_{F2} and S_{F3} is restricted to only one anthryl group, which is supposed to be planar. With this in mind, we suggest that, for example, S_{F2} emerges from S_{F1} by keeping group 1 fully planar and the C(9)−C(9′) bond fixed in space, but folding group 2 along the line through C(9′) and C(10′) in the manner encountered in the case of the photodimerization of anthracene. The original steric hindrance between hydrogen atoms is relieved in the resulting structure. This structure must be compared with the previously proposed structure of fluorescent BA in nonpolar solvents involving a twist angle of either 70° or 62°.[8,15,18] The latter geometries amount merely to a small deviation from a sphere and are incompatible with the observed long rotational relaxation time. The difference between the structure in S_{F3} and the suggested structure in S_{F2} may be attributed to a difference in the orientation of the deformed group 2, namely that one structure is obtained from the other by a 90° rotation of the deformed group 2 around the C(9)−C(9′) bond. Such a structural change is accompanied by small spectral shifts. As a result of the deformation, the partial dipole moments of the C−H bonds in group 2 do not cancel each other and the structures in the states S_{F2} and S_{F3} have a permanent dipole moment, which has nothing to do with electron transfer between the anthryl groups. The dielectric loss may be attributed to interconversion of the structures in the states S_{F2} and S_{F3} and is then a process involving nuclear motion rather electron hopping.

To the right of the dashed line in Figure 7, the time dependence of the signals for parallel and orthogonal polarization reflect the depolarization of the transition caused by rotational reorientation of the excited solute. Figure 8 compares the transient absorbance at magic angle polarization on a long time scale for two different wavelengths. There is a clear difference between the curves for 520 and 600 nm. The slow growth component at 520 nm is absent at 600 nm. The growth component has been found in the range 490−550 nm.

Based on this observation, the transient dielectric relaxation of the solution is attributed to interconversion of the structures

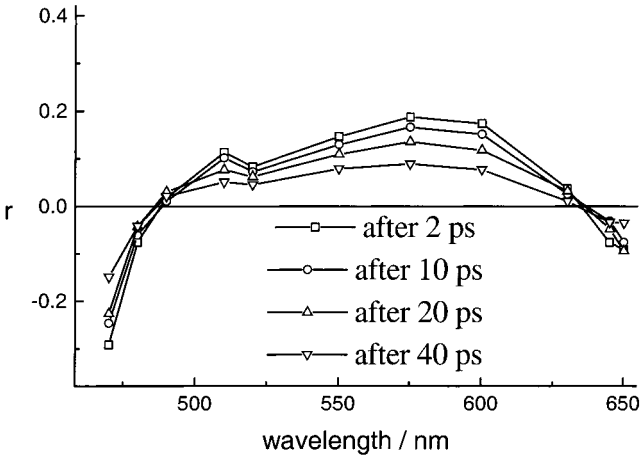

Figure 9. Anisotropy of the transient absorption of BA in cyclohexane at various wavelengths and at four different delay times.

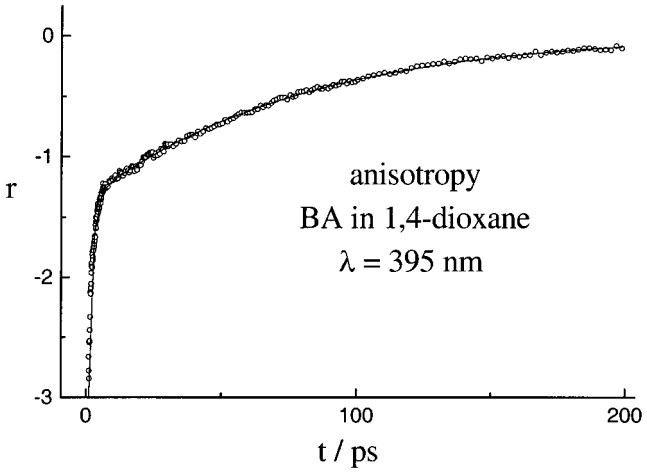

Figure 10. Time dependence of the anisotropy of the transient absorption of BA in 1,4-dioxane at 395 nm. The line through the data points represents the fitted biexponential function.

in S_{F2} and S_{F3}. Based on the absence of steric hindrance, the rate of interconversion is expected to be much faster than the decay of the very long-lived excited-state population. Consequently, the equilibrium between S_{F2} and S_{F3} is expected to be reached single exponentially with rate constant equal to the sum of the rate constants for the forward and the reverse reactions.

In the wavelength region $490 \leq \lambda \leq 550$ nm, where the growth with time constant of 9.8 ps in the transient absorbance is observed at magic angle polarization, the evolution of the anisotropy of the same absorbance is not exhibiting a growth component. This behavior is to be expected when the suggestions concerning states S_{F2} and S_{F3} are true. The growth at magic angle polarization corresponds to the transfer of population in state S_{F1} to the populations of S_{F2} and S_{F3}. Since group 1 is the excited chromophore in both state S_{F2} and state S_{F3}, their interconversion does not alter much in the transient absorption spectrum. Consequently, the interconversion does not change the anisotropy of the combined transient absorptions of the chromophore with mutual perpendicular polarization.

The anisotropy of the transient absorption in the wavelength range $470 \leq \lambda \leq 650$ nm is shown in Figure 9 for a number of selected times. The decay of the anisotropy of the transient absorptions is found to be independent of wavelength and to be monoexponential with a time constant of 49 ± 1 ps. Note that the anisotropy is positive and smaller than 0.4 as a function of time in the range $486 < \lambda < 637$ nm, is zero and independent of time at 486 and 637 nm, and is negative as a function of time at $\lambda < 486$ nm and at $\lambda > 637$ nm. The time independence and vanishing of the anisotropy at 486 and 637 nm indicates that contributions of several transitions with different directions of their transition moments are being canceled in the anisotropy at these two wavelengths. The values $0 \leq r(0) < 0.4$ in the range $486 < \lambda < 637$ nm can be attributed to overlap of absorption bands for which the transition moments have different directions. The peak in the transient absorption appears at 575 nm[12] and must be dominated by a transition polarized parallel to the polarization of the ground state absorption. Previously the polarization of the transient absorbances at 550 and 575 nm have been reported[12] to be mutually perpendicular. This is in contradiction to our finding that there is overlap of bands with different polarizations at both wavelengths, but with the parallel polarization dominant. The value $r(0) = -0.25$ for the transient absorbance at 470 nm is slightly more negative than the value -0.2 for an isolated transition with polarization perpendicular to that of the pump transition and may be regarded as the result of the contribution of stimulated emission with polarization parallel to the pump transition.

Both the interconversion of the structures in S_{F2} and S_{F3} and their rotational diffusion will contribute to dielectric loss, but the fast rate of interconversion may make the former process the dominant loss mechanism. The dielectric relaxation may then exhibit nearly Debye behavior. Although the dielectric relaxation times of excited BA in benzene or 1,4-dioxane have been determined, under the assumption of Debye behavior, to be about 9.2 and 11.7 ps,[5] respectively, the very small difference with the time constant of 9.8 ps may be accidental, because there are indications of exciplex formation between these solvents and BA.[4] The participation of the equilibrium between excited solute and solvent as an additional fast dielectric relaxation mechanism will then result in non-Debye behavior.

2b. Solution in 1,4-Dioxane. The evolution of the anisotropy of the transient absorbance of BA in 1,4 dioxane at 395 nm is shown in Figure 10. The fluorescence spectrum of the solution exhibits only the normal fluorescence at this wavelength. Therefore, the contribution of stimulated emission to the signal in Figure 10 must arise from species (state S_{F1}) emitting normal fluorescence. A dramatic change in the magnitude of the contributed stimulated emission takes place in the first few picoseconds and causes the appearance of a fast component in the anisotropy of the transient absorbance. The time dependence of the anisotropy in Figure 10 can be represented as a biexponential function with the time constants equal to 1.4 ± 0.2 ps and 77 ± 2 ps. Since the time constant of 1.4 ± 0.2 ps is close to the value (1.6 ps) reported previously for the time constant of the growth of the anomalous fluorescence (state S_{FA}),[13] it can be identified with the time constant for the conversion of the state S_{F1} into the state S_{FA}. Since the populations of the states S_{F2} and S_{F3} have been found above to build up with a time constant of 9.8 ps, they can be ruled out as the precursors of the state S_{FA}. The time constant of 77 ps must be attributed to the depolarization of the monitored optical transition through rotational diffusion of species in state S_{FA}. However, it is likely that an equilibrium will be established between species in the states S_{FA}, S_{F2}, and S_{F3}. Then rotational diffusion of all three types of species will contribute to the depolarization. The time constant of the depolarization will then be somewhere between the values to be expected for the fastest and slowest rotating type alone. Note the significant difference between the time constant of 77 ps in the present case and τ_A in the case of the solution in cyclohexane (Table 3). To see if

TABLE 4: Simulation of Fluorescence Depolarization Kinetics for 9,9′-Bianthryl in 1,4-Dioxane Using the Geometry Optimized in the Case of the Solution in Cyclohexane

τ_{xp}/[ps]	τ_0/[ps]	τ_R/[ps]	$r(0)$	V/[Å^3]	η/[cP]	T/[K]
77 ± 2	2.4	74.6	0.4	330	1.2	295
a	b	Φ_1	γ_1/ps	Φ_2	γ_2/ps	
0.472	0.3655	0	4.7	0.4	59.5	

this difference may arise from the difference among the viscosities of the solvents, the value of τ_A is recalculated by using the value of the viscosity of 1,4-dioxane. The result, presented in Table 4, yields a scaled value $\tau_A = 59.5$ ps, which is substantially smaller than the experimental value of 77 ps. This suggests that species in the state S_{FA} in the solution in 1,4-dioxane are larger in size than the species detected in the solution in cyclohexane. The suggestion supports the explanation of the anomalous fluorescence in terms of solute−solvent exciplexes. In other words, species in the state S_{FA} are solute−solvent exciplexes (*E*).

2c. Solution in Propionitrile. Two previous observations concerning the solution of BA in cyclohexane are relevant for the discussion here.[4] The first one is that the fluorescence intensity of the solution of BA in cyclohexane is quenched linearly as a function of added small concentrations of propionitrile. The second one is that the ratio of the intensities of the anomalous and normal fluorescence varies linearly with the added concentration of propionitrile. These observations are reasons to attribute the anomalous fluorescence of BA in propionitrile to solute−solvent exciplexes (*E**).

The time dependence of the fluorescence intensity of the solution of BA in propionitrile is shown in Figure 11 for both parallel and perpendicular polarizations at 400 nm. Mainly normal type fluorescence is observed at this wavelength. Since the total fluorescence quantum yield (Φ_F(total)) is reduced by a factor of about 2.5 by changing from cyclohexane to propionitrile as solvent, the value at 400 nm, $\Phi_F(400)$, must be reduced by an even larger factor as the consequence of the conversion of species emitting in the normal fluorescence band (S_{F1} and the equilibrium between states S_{F2} and S_{F3}) in those emitting anomalous fluorescence (S_{FA}). As a result of the small value of $\Phi_F(400)$, the recorded anisotropy $r_F(t)$ has a very poor signal-to-noise ratio. However, at $t = 0$, when the fluorescence intensity at 400 nm has its maximum value, a reliable value $r_F(0)$ can be calculated. This amounts to $r_F(0) = 0.4$. This is a result encountered also in the case of the fluorescence of the solution in cyclohexane. There is a decay during the first 5 ps of the evolution of $r_F(t)$ at 400 nm which is faster than expected for a change arising from rotational diffusion. Unfortunately the value of $\Phi_F(400)$ is too small to enable the determination of its time constant. However, $\Phi_F(520)$ is larger, and $r_F(t)$ at 520 nm is showing a growth from about 0.25 to 0.33 within this time window of 5 ps. By fitting curves to the noisy intensity traces for parallel and perpendicular polarized fluorescence at 520 nm, a reliable curve $r_F(t)$ could be calculated from them. This curve shown in Figure 12 yields a rough but significant value of 1.2 ps for the time constant of the growth component. Obviously, the growth in $r_F(t)$ at 520 nm is arising from the direct conversion of state S_{F1} into state S_{FA} and is in good agreement with the previously reported time constant of 1.4 ps for the growth of the anomalous fluorescence of BA in propionitrile.[13] Species in the state S_{FA} may be regarded here also as solute−solvent exciplexes *E**, as in the case of the solution of BA in 1,4-dioxane. The establishment of an equilibrium between species in the states S_{FA}, S_{F2}, and S_{F3} is very likely in the present case and this may be the reason $r_F(t)$ rises to a positive maximum value of less than 0.4. If only species in state S_{FA} were present after completion of the conversion of species in state S_{F1} a maximum value of either 0.4 or −0.2 is to be expected for the fluorescence anisotropy $r_F(t)$ in the time domain where rotational diffusion is negligible, because a single electronic transition is involved.

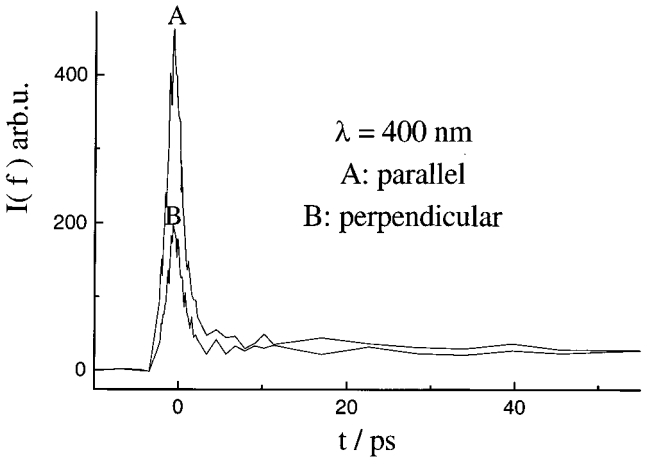

Figure 11. Time dependence of the fluorescence intensity of BA in propionitrile at 400 nm observed with polarization either parallel or perpendicular relative to the polarization of the pump beam.

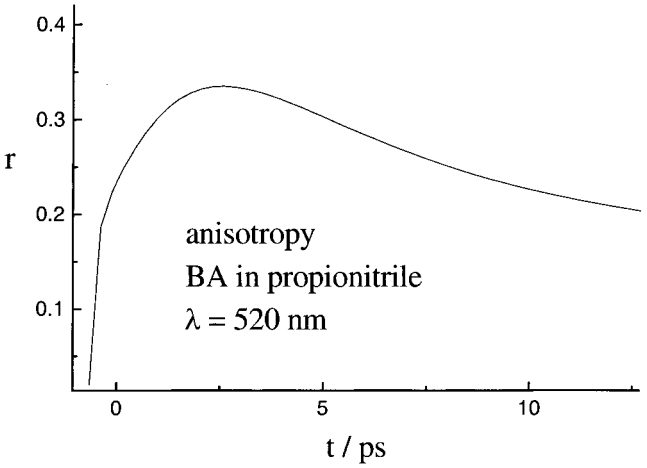

Figure 12. Time dependence of the anisotropy of the fluorescence of BA in propionitrile at 520 nm, derived from the functions fitted to the observed noisy signals for parallel and perpendicular polarization.

The transient absorbances at 550 and 760 nm in the early stage are shown in Figure 13. A decay component appears at 550 nm, while a growth component can be seen at 760 nm. These components have the same time constant, which amounts to 1.4 ps and may be attributed to the conversion of state S_{F1} into state S_{FA}, because the time constant is close in value to the rough value of 1.2 ps for the time constant of the growth component in $r_F(t)$ at 520 nm. The transient absorption yields a reliable value for the time constant of the conversion of state S_{F1}. This process manifests itself also in the anisotropies $r_A(t)$ of the transient absorbances at 600 and 690 nm, which are shown in Figure 14. The value of $r_A(t)$ at 600 nm remains positive all the time and decays single exponentially with a time constant of 1.4 ± 0.2 ps. This reflects the disappearance of species in state S_{F1}. The species emerging then exhibit optical absorption at 600 nm, but a slow component arising from their rotational diffusion does not appear in $r_A(t)$ at 600 nm. Apparently the absorbance at 600 nm gets depolarized completely in the course

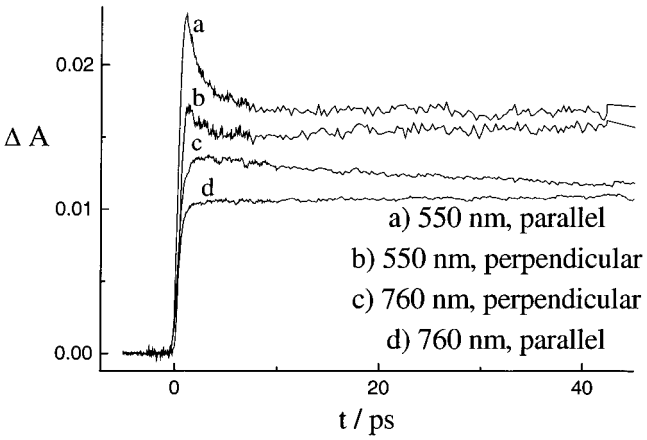

Figure 13. Time dependence of the transient absorbance of BA in propionitrile observed with either a parallel or perpendicular polarized probe beam and at 550 nm (two upper curves) and at 760 nm (two lower curves).

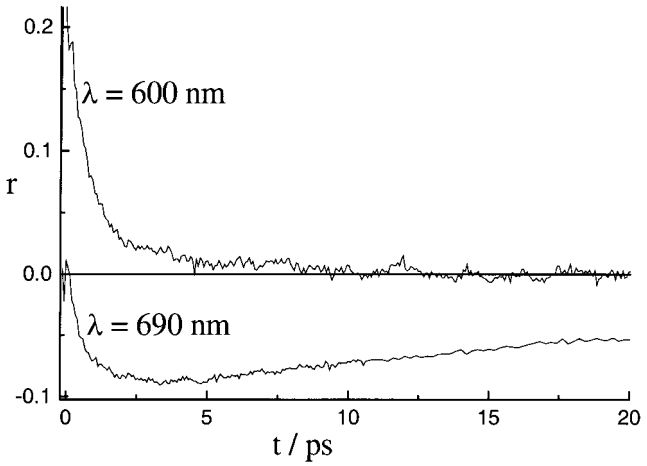

Figure 14. Time dependence of the anisotropy of the transient absorption of BA in propionitrile at 600 nm (upper curve) and at 690 nm (lower curve).

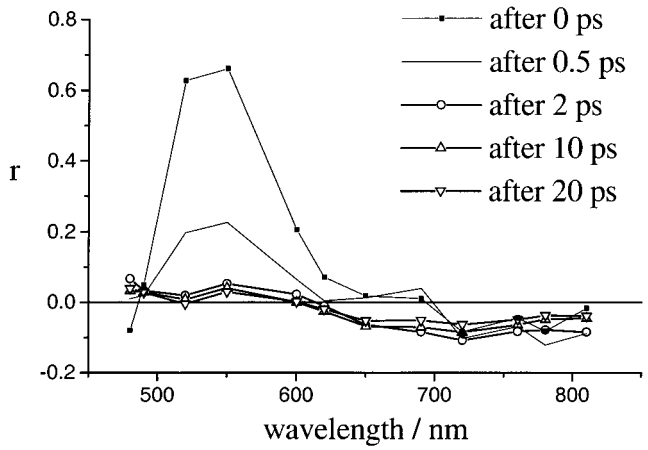

Figure 15. Anisotropy of the transient absorption of BA in propionitrile at various wavelengths at different delay times.

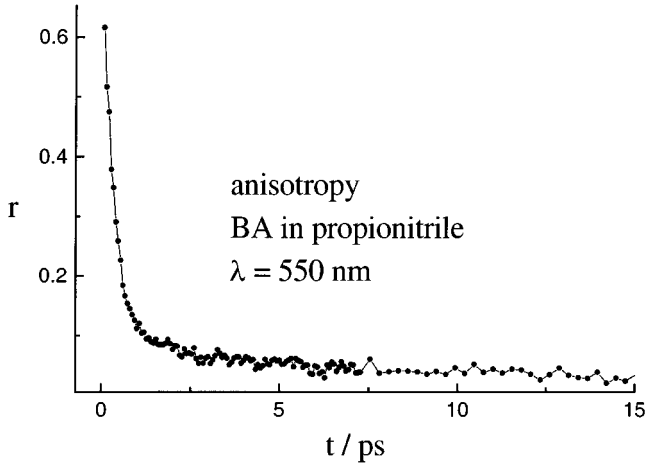

Figure 16. Time dependence of the anisotropy of the transient absorption of BA in propionitrile at 550 nm, showing biexponential decay with a fast component dominating in the beginning.

of the conversion of species in state S_{F1} and before the newly formed species have been subjected any significant rotational diffusion. Presumably, several types of species (e.g., in states S_{FA}, S_{F2}, and S_{F3}) are formed, among which both parallel and perpendicular polarizations may be encountered for their absorbance at 600 nm. In Figure 14 the value of $r_A(t)$ at 690 nm is nearly zero in the beginning and grows toward negative values with a time constant of 1.4 ± 0.2 ps and returns to zero with a long time constant of 29.9 ± 0.5 ps. Keep in mind that $r_A(0) \approx 0$ was obtained at 637 nm in the case of the solution in cyclohexane. Taking this into account and ruling out the possibility of large spectral shifts arising from differences in refractive indices of the solvents, the value of $r_A(0) \approx 0$ at 690 nm in the present case indicates that at least two different types of primary excited species are generated in the pump process and that their transition moments for the 690 nm transition are not mutually parallel. Let us refer to these two excited species as BA in the states S_{F1} and S_{FX}. Obviously the state S_{F1} in the present case may be identified with the state S_{F1} in the case of the solution in cyclohexane. The state S_{FX} must be considered as a primary excited state prepared by excitation of ground-state solute−solvent complexes of BA and propionitrile. The presence of such complexes in the solution may explain the remarkably large value of $r_A(0)$ appearing in Figure 15 around 550 nm. This value $r_A(0) \approx 0.6$ is substantially larger than the largest value (0.4) for linear absorption processes. This value may result from stimulated emission or nonlinear absorption by an excited species present in the solution at $t = 0$. We have to take into account that this type of species was not observed in the cases of the solutions in cyclohexane and that now anomalous fluorescence is appearing around 550 nm. Therefore, this type of species can be identified with an excited solute−solvent complex which loses energy during the pump process to enable stimulated emission around 550 nm at times close to $t = 0$. Figure 16 presents the decay of $r_A(t)$ at 550 nm, which can be represented as a biexponential function with time constants of 1.4 and 30 ps. Bearing the conclusion in mind that an equilibrium between excited solutes and solute−solvent exciplexes is established with a time constant of 1.4 ps, we arrive at the additional conclusion that excited solute−solvent complexes dissociate and get involved in this equilibrium with a time constant of at most 1.4 ps.

The fact that $r_A(t)$ in Figure 14 does not reach the value of −0.2 in the growth period means that several spectral bands are overlapping at 690 nm at the end of the growth, despite the disappearance of the population of S_{F1}. Apparently, the newly formed populations contribute both parallel and perpendicular components in the polarization of the absorbance at 690 nm. These may be populations of the states S_{FA}, S_{F2}, and S_{F3}, as in the case of the absorbance at 600 nm, but now a population of the radical cation of BA may also be involved. Assuming that the radical cation is not involved and that species in the states S_{FA}, S_{F2}, and S_{F3} are being interconverted rapidly, the shortest

TABLE 5: Simulation of Fluorescence Depolarization Kinetics for 9,9′-Bianthryl in Propionitrile Using the Geometry Optimized in the Case of the Solution in Cyclohexane

τ_{xp}/[ps]	τ_0/[ps]	τ_R/[ps]	$r(0)$	V/[Å^3]	η/[cP]	T/[K]
29.9 ± 0.5	2.4	27.5	0.4	330	0.42	295
a	b	Φ_1	γ_1/ps	Φ_2	γ_2/ps	
0.472	0.3655	0	1.7	0.4	20.8	

expected time constant for the slow component in $r_A(t)$ at 690 nm may be estimated. The estimated value of this time constant amounts to 20.8 + 2.4 = 23.2 ps (Table 5), which is 22% less than the experimental value of 29.9 ps. In the case of the solution in 1,4-dioxane mentioned above, the scaled value of 59.5 ps is also 22% less than the experimental value of 77 ps for decay of $r_A(t)$ at 395 nm. Since the solute−solvent exciplexes in the two solutions are not expected to have equal time constants for rotational diffusion and the relative difference between scaled and experimental time constants is the same for the two solutions, we conclude that the depolarization of the optical transition is predominantly controlled by rotational diffusion of species in the states S_{F2} and S_{F3} in both solutions. Since the radical cation has been shown to be formed and to absorb at 690 nm (at least in the solution in acetonitrile), it is either not formed prior to full depolarization of the absorption or its rotational diffusion is not much slower than that of the species in states S_{F2} and S_{F3}.

Conclusions

The first UV absorption band of solutions of anthracene turns out to cover two mutually perpendicularly polarized electronic transitions, whereas the first UV absorption band of 9,9′-bianthryl (BA) in alkanes arises from a single isolated electronic transition. Ground-state solute−solvent complexes appear in the solution of anthracene in 1,4-dioxane.

The presented discoveries imply that the transient dielectric relaxation of photoexcited solutions of BA in cyclohexane is arising from both a chemical equilibrium involving a deformed polar excited solute and rotational diffusion of the latter and cannot be expected to exhibit Debye behavior. The excited-state dipole moment may arise from lack of mutual cancellation of bond dipole moments after the deformation. Previous claims that a charge-transfer excited state of BA was observed are shown to be based on misinterpretations of the observations.

The finding that only one of the anthryl groups in BA is nonplanar after the structural deformation in the excited state implies that the primary excitation is causing redistribution of electrons in both anthryl groups. This in turn implies electron delocalization over both anthryl groups in the ground state molecule and therefore a twist angle between the two groups of substantially less than 90° in the ground state.

There is new evidence for the previous conclusion that the fluorescence of solutions of BA in alkanes is emitted from the primary excited-state S_{F1} and two secondary states S_{F2} and S_{F3} emerging from it. The formation of solute−solvent exciplexes upon UV excitation of solutions of BA in 1,4-dioxane and propionitrile is in agreement with several new results. Solute−solvent exciplexes are formed in the solution of BA in 1,4-dioxane by interaction of a solvent molecule and a solute in the state S_{F1}. The newly formed exciplexes get into equilibrium with solutes in the states S_{F2} and S_{F3} later on.

There is evidence that the solution of BA in propionitrile contains ground-state solute−solvent complexes which are converted into solute−solvent exciplexes upon UV excitation.

Appendix

The expressions[35] for Ω_j and γ_j appearing in eq 2 are presented here.

$$\Omega_1 = \frac{1}{15}(\beta + \alpha) \quad \gamma_1 = -(6D + 2\Delta) \tag{A1}$$

$$\Omega_2 = \frac{1}{15}(\beta - \alpha) \quad \gamma_2 = -(6D - 2\Delta) \tag{A2}$$

$$\Omega_3 = \frac{4}{15}(u_z u_x v_z v_x) \quad \gamma_3 = -3(D_y + D) \tag{A3}$$

$$\Omega_4 = \frac{4}{15}(u_y u_z v_y v_z) \quad \gamma_4 = -3(D_x + D) \tag{A4}$$

$$\Omega_5 = \frac{4}{15}(u_x u_y v_x v_y) \quad \gamma_5 = -3(D_z + D) \tag{A5}$$

$$I_S = \frac{1}{6}C(t) - \frac{1}{2}I_P \tag{A6}$$

with $C(t)$ the excited-state population and D_x, D_y, D_z the rotational diffusion constants for rotation around the x, y, z axes respectively and

$$\beta = (u_x^2 v_x^2 + u_y^2 v_y^2 + u_z^2 v_z^2) - \frac{1}{3} \tag{A7}$$

$$\alpha = \sum_{j=1}^{4} \Lambda_j \tag{A8}$$

where

$$\Lambda_1 = \frac{D_x}{\Delta}(u_y^2 v_y^2 + u_z^2 v_z^2 - 2u_x^2 v_x^2 + u_x^2 + v_x^2) \tag{A9}$$

$$\Lambda_2 = \frac{D_y}{\Delta}(u_z^2 v_z^2 + u_x^2 v_x^2 - 2u_y^2 v_y^2 + u_y^2 + v_y^2) \tag{A10}$$

$$\Lambda_3 = \frac{D_z}{\Delta}(u_x^2 v_x^2 + u_y^2 v_y^2 - 2u_z^2 v_z^2 + u_z^2 + v_z^2) \tag{A11}$$

$$\Lambda_4 = -\frac{2D}{\Delta} \tag{A12}$$

with

$$D = \frac{1}{3}(D_x + D_y + D_z) \tag{A13}$$

$$\Delta = \{(D_x^2 + D_y^2 + D_z^2 - D_x D_y - D_y D_z - D_z D_x)\}^{1/2} \tag{A14}$$

These relations yield the following expression:

$$I_P(t) - I_S(t) = \frac{3}{2}C(t)\sum_{j=1}^{5}\Omega_j \exp(-\gamma_j t) \tag{A15}$$

$$I_P(t) + 2I_S(t) = \frac{1}{3}C(t) \tag{A16}$$

When both the pump and probe processes involve single

electronic transitions, one obtains

$$r(t) = \sum_{j=1}^{5} \Phi_j \exp(-\gamma_j t) \quad \text{(A17)}$$

where

$$\Phi_1 = \frac{3}{10}(\beta + \alpha) \quad \text{(A18)}$$

$$\Phi_2 = \frac{3}{10}(\beta - \alpha) \quad \text{(A19)}$$

$$\Phi_3 = \frac{6}{5}(u_z u_x v_z v_x) \quad \text{(A20)}$$

$$\Phi_4 = \frac{6}{5}(u_y u_z v_y v_z) \quad \text{(A21)}$$

$$\Phi_5 = \frac{6}{5}(u_x u_y v_x v_y) \quad \text{(A22)}$$

Consider the special case in which the probe process involves a single electronic transition, but the pump process involves two electronic transitions with probabilities f_1 and f_2. The signal I_P consists then of contributions I_{P1} and I_{P2}, arising from the first and second electronic transition in the pump process, respectively. Similarly I_S consists of contributions I_{S1} and I_{S2}. Then $r(t)$ is given by

$$r(t) = \frac{(I_{P1} + I_{P2}) - (I_{S1} + I_{S2})}{(I_{P1} + I_{P2}) + 2(I_{S1} + I_{S2})} \quad \text{(A23)}$$

Using the relation $f_2 = pf_1$ for the relative magnitudes of the transition probabilities, one obtains

$$r(t) = \frac{1}{1 + p} \sum_{j=1}^{5} (\Phi_{1j} + p\Phi_{2j}) \exp(-\gamma_j t) \quad \text{(A24)}$$

where

$$\Phi_{11} = \frac{3}{10}(\beta_1 + \alpha_1) \quad \Phi_{21} = \frac{3}{10}(\beta_2 + \alpha_2) \quad \text{(A25)}$$

$$\Phi_{12} = \frac{3}{10}(\beta_1 - \alpha_1) \quad \Phi_{22} = \frac{3}{10}(\beta_2 - \alpha_2) \quad \text{(A26)}$$

$$\Phi_{13} = \frac{6}{5}(u_{1z} u_{1x} v_z v_x) \quad \Phi_{23} = \frac{6}{5}(u_{2z} u_{2x} v_z v_x) \quad \text{(A27)}$$

$$\Phi_{14} = \frac{6}{5}(u_{1y} u_{1z} v_y v_z) \quad \Phi_{24} = \frac{6}{5}(u_{2y} u_{2z} v_y v_z) \quad \text{(A28)}$$

$$\Phi_{15} = \frac{6}{5}(u_{1x} u_{1y} v_x v_y) \quad \Phi_{25} = \frac{6}{5}(u_{2x} u_{2y} v_x v_y) \quad \text{(A29)}$$

$$\beta_1 = (u_{1x}^2 v_x^2 + u_{1y}^2 v_y^2 + u_{1z}^2 v_z^2) - \frac{1}{3} \quad \text{(A30)}$$

$$\beta_2 = (u_{2x}^2 v_x^2 + u_{2y}^2 v_y^2 + u_{2z}^2 v_z^2) - \frac{1}{3} \quad \text{(A31)}$$

$$\alpha_1 = \sum_{j=1}^{4} \Lambda_{1j} \quad \text{(A32)}$$

$$\alpha_2 = \sum_{j=1}^{4} \Lambda_j \quad \text{(A33)}$$

where

$$\Lambda_{11} = \frac{D_x}{\Delta}(u_{1y}^2 v_y^2 + u_{1z}^2 v_z^2 - 2u_{1x}^2 v_x^2 + u_{1x}^2 + v_x^2) \quad \text{(A34)}$$

$$\Lambda_{21} = \frac{D_x}{\Delta}(u_{2y}^2 v_y^2 + u_{2z}^2 v_z^2 - 2u_{2x}^2 v_x^2 + u_{2x}^2 + v_x^2) \quad \text{(A35)}$$

$$\Lambda_{12} = \frac{D_y}{\Delta}(u_{1z}^2 v_z^2 + u_{1x}^2 v_x^2 - 2u_{1y}^2 v_y^2 + u_{1y}^2 + v_y^2) \quad \text{(A36)}$$

$$\Lambda_{22} = \frac{D_y}{\Delta}(u_{2z}^2 v_z^2 + u_{2x}^2 v_x^2 - 2u_{2y}^2 v_y^2 + u_{2y}^2 + v_y^2) \quad \text{(A37)}$$

$$\Lambda_{13} = \frac{D_z}{\Delta}(u_{1x}^2 v_x^2 + u_{1y}^2 v_y^2 - 2u_{1z}^2 v_z^2 + u_{1z}^2 + v_z^2) \quad \text{(A38)}$$

$$\Lambda_{23} = \frac{Dz}{\Delta}(u_{2x}^2 v_x^2 + u_{2y}^2 v_y^2 - 2u_{2z}^2 v_z^2 + u_{2z}^2 + v_z^2) \quad \text{(A39)}$$

$$\Lambda_{14} = \Lambda_{41} = -\frac{2D}{\Delta} \quad \text{(A40)}$$

with

$$D = \frac{1}{3}(D_x + D_y + D_z) \quad \text{(A41)}$$

$$\Delta = \{(D_x^2 + D_y^2 + D_z^2 - D_x D_y - D_y D_z - D_z D_x)\} \quad \text{(A42)}$$

References and Notes

(1) Schneider, F.; Lippert, E. *Ber. Bunsen-Ges. Phys. Chem.* **1968**, *72*, 1155.
(2) Liptay, W.; Walz, G.; Baumann, W.; Schlosser, H. J.; Deckers, H.; Detzer, N. *Z. Naturforsch.* **1971**, *26a*, 2020.
(3) Liptay, W.; Schlosser, H. J. *Z. Naturforsch.* **1972**, *27a*, 1336.
(4) Visser, R. J.; Weisenborn, P. C. M.; van Kan, P. J. M.; Huizer, A. H.; Varma, C. A. G. O.; Warman, J. M.; de Haas, M. P. *J. Chem. Soc., Faraday Trans. 2*, **1985**, *81*, 689.
(5) Toublanc, D. B.; Fessenden, R. W.; Hitachi, A. *J. Phys. Chem.* **1989**, *93*, 2893.
(6) Baumann, W.; Spohr, E.; Bischof, H.; Liptay, W. *J. Lumin.* **1987**, *37*, 227.
(7) Wortmann, R.; Lebus, S.; Kartsen, E.; Assar, S.; Detzer, N.; Liptay, W. *Chem. Phys. Lett*. **1992**, *198*, 220.
(8) Grabner, G.; Rechthaler, K.; Köhler, G. *J. Phys. Chem. A* **1998**, *102*, 689.
(9) Laguitton-Pasquier, H.; Pansu, R.; Chauvet, J. P.; Collet, A.; Faure, J.; Lapouyade, R. *Chem. Phys*. **1996**, *212*, 437.
(10) Rettig, W.; Zander, M. *Ber. Bunsen-Ges. Phys. Chem*. **1983**, *87*, 1143.
(11) Zander, M.; Rettig, W. *Chem. Phys. Lett*. **1984**, *110*, 602.
(12) Lueck, H.; Windsor, M. W.; Rettig, W. *J. Phys. Chem.* **1990**, *94*, 4551.
(13) Kang, T. J.; Kahlow, M. A.; Giser, D.; Swallen, S.; Nagarajan; V.; Jarzeba, W.; Barbara, P. F. *J. Phys. Chem*. **1988**, *92*, 6800.
(14) Kang, T. J.; V.; Jarzeba, W.; Barbara, P. F. *Chem. Phys*. **1990**, *149*, 81.
(15) Mataga, N.; Nishikawa, S.; Okada, T. *Chem. Phys. Lett*. **1996**, *257*, 327.

(16) Subaric-Letis, A.; Monte, CH.; Roggan, A.; Rettig, W.; Zimmermann, P. J. *Chem. Phys*. **1990**, *93*, 4543.
(17) Elich, K.; Kitazawa, M.; Okada, T.; Wortmann, R. *J. Phys. Chem. A* **1997**, *101*, 2010.
(18) Wortmann, R.; Elich, K.; Lebus, S.; Liptay, W. *J. Chem. Phys.* **1991**, *95*, 6371.
(19) Grabowski, Z. R.; Rotkiewicz, K.; Siemiarczuk, S.; Cowley, D. L.; Baumann, W. *Nouv. J. Chim.* **1979**, *3*, 443.
(20) Chandross, E. A. In *The Exciplex*; Gordon, M., Ware, R., Eds.; Academic Press: New York, 1975.
(21) Visser, R. J.; Varma, C. A. G. O. *J. C. S. Faraday Trans. 2*, **1980**, *76*, 453.
(22) Visser, R. J.; Weisenborn, P. C. M.; Varma, C. A. G. O. *Chem. Phys. Lett*. **1985**, *113*, 330.
(23) De Lange, M. C. C.; Thorn Leeson, D.; Van Kuijk, K. A. B.; Huizer, A. H.; Varma, C. A. G. O. *Chem. Phys.* **1993**, *174*, 425.
(24) De Lange, M. C. C.; Thorn Leeson, D.; Van Kuijk, K. A. B.; Huizer, A. H.; Varma, C. A. G. O. *Chem. Phys.* **1993**, *177*, 243.
(25) Ishida, T.; Fujimura, Y.; Fujiwara, T. Kajimoto, O. *Chem. Phys. Lett.* **1998**, *288*, 433.
(26) Nishiyama, K.; Honda, T.; Okada, T. *Acta Phys. Pol*. **1998**, *94*, 847.
(27) Okada, T.; Nishikawa, S.; Kanaji, K.; Mataga, N. In *Ultrafast Phenomena VII, Springer Series in Chemical Physics*, Vol. 53; Harris, C. B., Ippen, E. P., Mourou, G. A., Zewail, A. H., Eds.; Springer: Berlin, 1990.
(28) Mataga, N.; Yao, H.; Okada, T.; Rettig, W. *J. Phys. Chem*. **1989**, *93*, 3383.
(29) Bowen, E. J. *Adv. Photochem*. **1963**, *1*, 23.
(30) Wan, J. K. S.; McCormick, R. N.; Baum, E. J.; Pitts, J. N., Jr. *J. Am. Chem. Soc*. **1965**, *87*, 4409.
(31) Chandross, E. A.; Ferguson, J.; McRae, E. G. *J. Chem. Phys*. **1966**, *45*, 3546.
(32) Birks, J. B. In *The Exciplex*; Gordon, M., Ware, R., Eds.; Academic Press: New York, 1975.
(33) Buma, W. J.; Groenen, E. J. J.; Schmidt, J. *J. Chem. Phys*. **1989**, *91*, 6549.
(34) de Bekker, E. J. A.; Pugzlys, A.; Varma, C. A. G. O. *J. Chem. Phys*. **2001**, *105*, 399.
(35) Chuang, T. J.; Eisenthal, K. B. *J. Chem. Phys.* **1972**, *57*, 5094.
(36) Herring, F. G.; Philips, P. S. *J. Chem. Phys.* **1980**, *73*, 2603.
(37) Lettenberger, M.; Emmerling, F.; Gottfried, N. H.; Laubereau, A. *Chem. Phys. Lett*. **1995**, *240*, 324.
(38) Bauer, D. R.; Brauman, J. I.; Pecora, R. *J. Am.Chem. Soc*. **1974**, *96*, 6840.
(39) Williams, A. M.; Jiang, Y.; Ben-Amotz, D. *Chem. Phys.* **1994**, *180*, 119.
(40) Benzler, J.; Luther, K. *Chem. Phys. Lett*. **1997**, *279*, 333.
(41) Evans, G. T.; Kivelson, D. *J. Chem. Phys.* **1986**, *84*, 385.
(42) Youngren, G. K.; Acrivos, A. *J. Chem. Phys*. **1975**, *63*, 3846.
(43) Sension, R. J.; Hochstrasser, R. M. *J. Chem. Phys.* **1993**, *98*, 2490.
(44) Dorfmüller, Th. Daum, B. Hanschmidt, A. *J. Chem. Phys*. **1991**, *95*, 813.
(45) Jas, G. S.; Wang, Y.; Pauls, S. W.; Johnson, C. K.; Kuczera, K. *J. Chem. Phys*. **1997**, *103*, 8800.
(46) Berlman, I. B. *Handbook of Fluorescence Spectra of Aromatic Molecules*, 2nd ed; Academic Press: New York and London, 1971.